We are IntechOpen, the world's leading publisher of Open Access books Built by scientists, for scientists

4,800
Open access books available

122,000
International authors and editors

135M
Downloads

Our authors are among the

154
Countries delivered to

TOP 1%
most cited scientists

12.2%
Contributors from top 500 universities

CLARIVATE ANALYTICS BOOK CITATION INDEX INDEXED

WEB OF SCIENCE™

Selection of our books indexed in the Book Citation Index in Web of Science™ Core Collection (BKCI)

Interested in publishing with us?
Contact book.department@intechopen.com

Numbers displayed above are based on latest data collected.
For more information visit www.intechopen.com

16

Pharmacokinetic/Pharmacodynamic (PK/PD) Modeling of Anti-Neoplastic Agents

Daniel Lexcen[1], Ahmed Salem[2],
Walid M. El-Khatib[3], Virginia Haynes[4] and Ayman Noreddin[5,*]
[1]*University of Minnesota*
[2]*Abbott Co Ltd.*
[3]*Ain-Shams University*
[4]*Lake Superior College*
[5]*Hampton University*
USA

1. Introduction

Development of tumor resistance to chemotherapeutics is related to inherent tumor variations regarding sensitivity to chemotherapeutics and to sub-optimal dosing regimens, including variation in patient pharmacokinetics that result in suboptimal exposure of tumor cells to anti-neoplastic drugs [1, 2]. The rate and extent of drug efficacy depends on the extent of drug exposure at the tumor site and the time above the effective concentration [3]. *In vitro* models that incorporate these pharmacokinetic and pharmacodynamic (PK/PD) principles to optimize therapeutic response may be considered the method of choice for optimizing dosing schedules before translating data from static assays to animals and clinical trials [4, 5]. The hollow fiber bioreactor was recently used to evaluate pharmacokinetic/pharmacodynamic (PK/PD) effects of gemcitibine in lung and breast cancers and to model HIV treatments [4-6].

2. Hollow fiber bioreactor model

The hollow fiber bioreactor model (Figure 1) is a dynamic system that provides a cell culture with constant flow of fresh medium through a 3D polysulfone cartridge (support for cell growth) with capillary sized passages (cells grow in the extracapillary space), at physiologically relevant flow rates. Automatic programmable pumps accurately regulate dosing of chemotherapeutics into the system.

The hollow fiber cartridge consists of two compartments, the porous capillaries through which medium flows and the extra-capillary space (ECS) that separates the cell culture from the flowing medium. Medium is constantly perfused through the fibers into the ECS, carrying nutrients and infused drugs to the cell culture. Due to the dynamic nature of the

* Corresponding Author

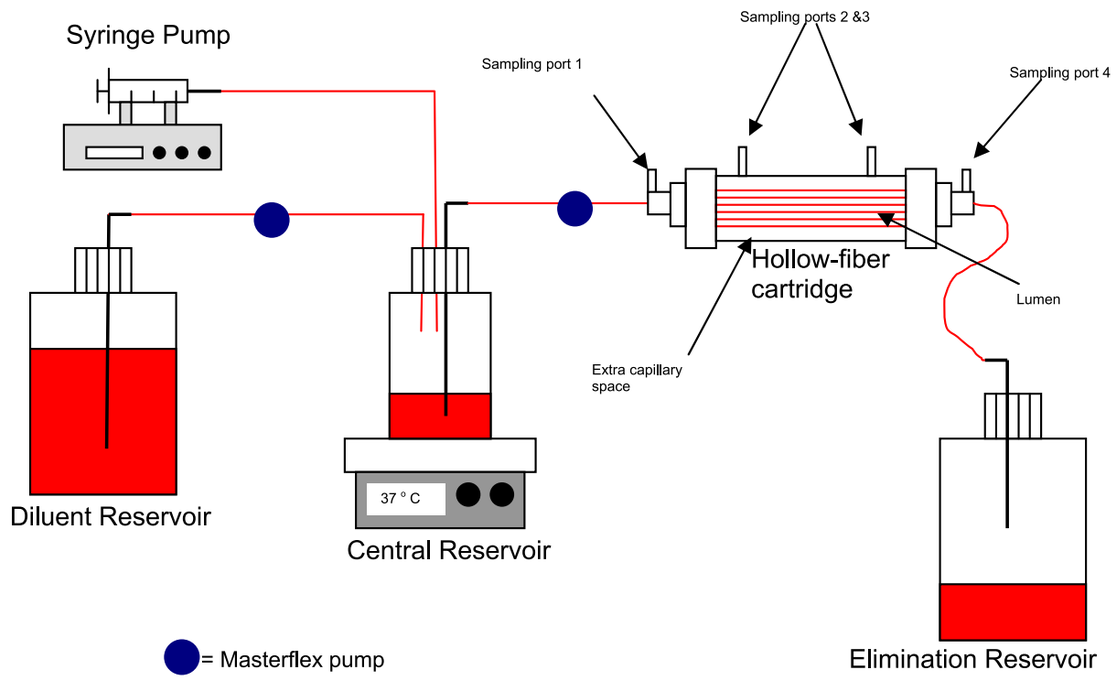

Fig. 1. Schematic of the bioreactor setup

model, cells can be exposed to carefully chosen drug concentrations that simulate patient pharmacokinetics from published clinical data, simulating drug half-life and renal clearance [6]. This change in concentration over time cannot be achieved in static assays. To monitor cell growth and viable counts in undisturbed hollow fiber cultures, we used an assay based on measurement of fluorescence resulting from the reduction of non-fluorescent resazurin to its red fluorescent form (resorufin) by metabolically active cells [7]. The intensity of the fluorescence is proportional to the viable cell count [8]. Achievement of cell cycle arrest, as a surrogate marker of the therapeutic outcome, was measured by flow cytometry. We hypothesized that we could use the proposed dynamic model to accurately simulate (*R*)-roscovitine (ROSC) pharmacodynamics, incorporating pharmacokinetic data. To achieve this, we used the MCF-7 human breast cancer cell line and compared the peak values from two proposed dosing regimens of ROSC to untreated controls.

MCF-7 cells are derived from the pleural effusion of an estrogen receptor positive, human breast adenocarcinoma [9, 10]. Cells were cultured in EMEM, 2mM L-glutamine, 0.1mM non-essential amino acids, 1mM sodium pyruvate, 0.01mg/mL bovine insulin and 10% fetal bovine serum; grown in 5% CO_2 at 37° C and dispersed when confluent with of 0.25% trypsin/0.5mM EDTA. Hollow fiber cartridges were prepared according to manufacturers instructions. To prepare hollow fiber cultures, briefly, trypsinized cells were diluted to 1.67 x 10^6/mL; 3mL were seeded into the ECS of each cartridge. Two cartridges were seeded for each experiment; one for drug treatment and one control. Cartridges were placed on a dual recirculating pump in the incubator at 37°C with 5% CO_2 to circulate fresh sterile medium to each cartridge simultaneously while establishing the cultures.

2.1 Pharmacokinetic simulation for (R)-roscovitine

After 24 hours, cartridges were removed from the recirculating pump, connected to a linear pump system (Masterflex) and a digital syringe pump was used to control the rate of drug infusion (Figure 1). Mathematical pharmacokinetic drug profiles were simulated by adjusting the input of ROSC and medium in the system. Infusion of the drug at peak concentration was followed by simulation of its clearance rate over a 6 hour period. Controls were perfused with drug free medium under the same conditions. Each dosing schedule was performed at least in duplicate.

2.2 PK/PD simulation for the bioreactor

A one compartment model, oral absorption and first order elimination was constructed using STELLA software (isee systems inc., Lebanon, NH). This model simulated pharmacokinetic profiles of peak and trough plasma levels after 800 mg twice daily (BID) and three times daily (TID) dosage regimens using pharmacokinetic parameters from a previously published clinical trial [11]. STELLA simulation provided a profile range of several C_{max} from which to mimic the C_{ss} (steady state concentration) in the bioreactor. To accomplish this infusion, peak and trough concentrations of the C_{ss} range were used to determine the final dose, which represented the population pharmacokinetics and was infused to the central reservoir. Simulated BID peak and trough concentrations were 3167 ng/mL and 808 ng/mL, respectively. Simulated TID peak and trough concentrations were 3893 ng/mL and 1923 ng/mL, respectively. Flow rates for the pumps were determined using the following equation for oral administration:

$$Cl = k_e \bullet V_d \tag{1}$$

$$k_e = \frac{Cl}{V_d} = \frac{\ln(\frac{C_1}{C_2})}{} = \frac{\ln C_1 - \ln C_2}{(t_2 - t_1)} \tag{2}$$

where C_l is clearance of drug and is equal to the rate set on the Masterflex pumps, k_e is the elimination rate constant for ROSC, V_d is central reservoir volume, C_1 is C_{max} from the simulation during the steady state, C_2 is C_{min} from the simulation during the steady state, and t (time) is the experiment duration. The rate of the digital pumps simulated the patient drug clearance.

2.3 LC/MS

To confirm the achievement of peak drug concentrations, samples were collected from the ECS of the hollow fiber cartridge and analyzed by LC/MS. The system included two Shimadzu LC- 20AD pumps, SIL-20AC autosampler, 2010 EV mass spectrometer with cosense module. A BDS Hypersil C18 (30mm x 2.1mm x 3µm) analytical column was used in conjunction with the co-sense system fitted with a Shimadzu MAYI-ODS 10L x 4.6 column. Mobile phase; A (10% ACN/ 90%, 0.1% Formic Acid) v/v and B (80% ACN and 20%, 0.1% Formic Acid) v/v; gradient at 50 % B increasing to 100% B over 1 min and remained isocratic at 100% B for 6 minutes until returning to 50% B. Flow rate was 0.150 ml/min with detection wavelength of 292 nm with an injection volume of 10µL. Mass spectrometry peaks

were analyzed using Shimadzu's data analysis program. Peak integrations were compared to a standard curve to obtain the concentrations of ROSC.

2.4 Resazurin assay

Fluorescent conversion of resazurin is directly related to the number of metabolically active cells in culture and serves as a surrogate probe for viable cell count. Medium containing 5% v/v resazurin was added to the hollow fiber system and circulated for 30 minutes for homogenous distribution of resazurin containing medium. System valves were closed and the cartridge incubated 2 hours; 200 µl samples were drawn from medium in the ECS. Fluorescence was measured on a microplate reader (Biotek, Winooski, VT). Resazurin was removed by pumping fresh medium through the system with linear pumps, collecting the resazurin medium as waste. Assays were performed before and after treatment for assessing baseline fluorescence and the effect of drug on cell proliferation. Resazurin has been reported to be cytotoxic at high concentrations and exposure beyond 24 hours [12]. Since cell lines respond differently to resazurin, [13], we conducted a static assay to establish that 5% (v/v) resazurin could be used over at least a 24 hour period without toxicity to the MCF-7 cell line. Cells incubated with resazurin, and untreated controls, were harvested, stained with trypan blue and counted at the conclusion of the experiment. This confirmed that growth and viability were unaffected by resazurin at 5% v/v (unpublished data).

2.5 Flow cytometry

MCF-7 cells were harvested from the hollow fiber cartridge by trypsinization and centrifuged at 300x g for 5 minutes. Supernatant was removed and the pellet resuspended in 0.5ml of PBS-T with 20 µg/mL of RNAse and incubated at 37°C for 30 min. 10µg/ml propidium iodide was added to the cell suspension and incubated at 37°C for 30 min. The stained nuclei (200,000 per sample) were analyzed with a Becton Dickinson FACSCalibur (San Jose, California) flow cytometer using medium flow mode. Cell cycle distribution was analyzed with Modfit LT program (Verity, Maine).

3. Results

Pharmacokinetic simulation of ROSC was used to predict the C_{max} of BID and TID dosing regimens. The predicted bolus dose values for the BID and TID were 3167ng/mL (8.9µM) and 3893ng/mL (10.9µM), respectively. From this data, we modeled a one dose peak profile that we could assess in the *in vitro* hollow fiber model. Actual concentrations of ROSC achieved in the model reached a C_{max} of 2953 ng/mL (8.3µM) for the BID schedule, an accuracy of 93.2% compared to the predicted value. Actual concentration for the TID schedule was 3307ng/mL (9.3µM) as compared to the mathematical profile C_{max} of 3893ng/mL, an accuracy of 85.0%. This level of accuracy for infused drug is consistent with the reports of Kirstein, et al. in their PK/PD studies in the hollow fiber model [5, 6]. To monitor cell proliferation and viability before treatment, without disturbing established cultures, we used the resazurin assay on all cartridges. There was no significant difference in cell proliferation between cartridges before treatment (p=0.86), indicating consistency in seeding the hollow-fiber cartridges. In post-treatment resazurin assays, ROSC treated cartridges had decreased cell proliferation compared to control cartridges. The TID (9.3µM) simulated dose had a 15-20% decrease in growth that was not evident with the BID (8.3 µM)

simulated dose (Figure 2). To determine the effect of ROSC on cell cycle, cells were collected by trypsinization from the hollow-fiber cartridge at 24 hours post-treatment and analyzed by flow cytometry. An increase was seen in the proportion of cells in the G1 phase in both the BID and TID treatments compared to the control. Correspondingly, there was a statistically significant decrease of the proportion of S phase cells in both the TID (p=0.004) and BID (p=0.003) doses compared to the control and a statistically significant increase in G2 for BID simulation (Table 1).

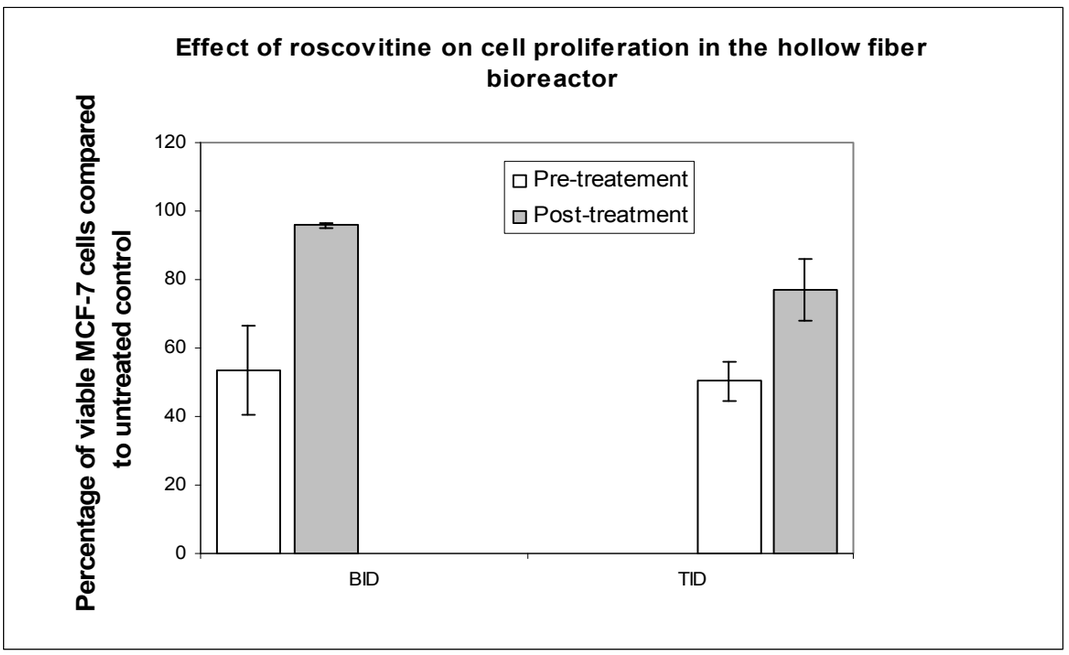

Fig. 2. Evaluation of cell proliferation in undisturbed cultures in the hollow fiber cartridge. Samples were taken for each set of cartridges for each experiment (n=2). A sample was taken from each cartridge before treatment (n=6). ROSC was infused at steady state value and clearance rate was simulated over 6 hours. Sample was taken at 24 hours (18 hours after infusion). Fluorescence was quantified as RFU and all values were normalized to the untreated control (final average value as 100%).

	G1 (%)	S (%)	G2 (%)
Control (n=5)	48.75 ± 3.71	33.93 ± 6.36	17.23 ± 2.68
BID (n=6)	54.51 ± 3.69	23.15 ± 1.89	22.34 ± 1.86
TID (n=5)	59.77 ± 3.86	22.49 ± 1.86	17.72 ± 5.55

n= number of experimental repetitions; BID 800mg twice daily; TID 800mg three times daily.

Table 1. Effect of ROSC dose increase on cell cycle distribution.
MCF-7 cells in each measured phase of growth cycle (G1, S or G2) are expressed as a percentage (± Standard Deviation) of the total number of cells.

4. Discussion

Uncontrolled proliferation is a defining characteristic of tumor cells. This is known to occur through mutation in genes that produce regulatory proteins which modulate cell cycle, such as the Cyclin Dependent Kinases (Cdks) [14-16]. Cdks are highly conserved serine/threonine kinases whose activation depends on formation of a heterodimeric complex with cyclins [17-19]. Thus, Cdks are a promising therapeutic target for cancer treatment [20]. ROSC is a novel Cdk inhibitor that induces cell cycle arrest and apoptosis through multiple intracellular targets in a variety of tumor cell lines. When tested in static *in vitro* assays, IC_{50} values of about 14μM are reported with 24 hours of drug exposure [21-24]. However, dosing schedules of 2500 mg/day over 5 days in 3 week cycles or the reduced dose of 1600mg/day BID for 10 days were recommended based on early human trials [25] and a concomitant Phase one trial that indicated a dose limiting toxicity of 800 mg BID for 7 days. With this dosing schedule, peak plasma levels were achieved in 1-4 hours with elimination by 2-5 hours. The highest plasma concentration achieved clinically was 10μM within a treatment period. There was no tumor response to this dose, although the disease was stabilized over several courses of treatment [11]. To investigate the effect of administration of ROSC as a monotherapy by altering the dosing schedule, we employed a dynamic hollow fiber model in this study. We established our model using STELLA to simulate pharmacokinetic profiles of ROSC derived from clinical data. These profiles were simulated in the *in vitro* hollow fiber model for assessing the effectiveness of two dosing regimens against MCF-7 cells by using flow cytometry to measure cell cycle distribution under each condition. The results revealed increasing numbers of MCF-7 cells accumulating in G1 phase after simulating the BID and TID dosing peaks with ROSC, and indicating a significant difference between TID and the control. Also, BID dosing simulation had a significant increase in G2 arrest ($p<0.05$). This data is consistent with previous studies which indicated arrest of MCF-7 cell proliferation at the G1/S transition and G2/M transition with accumulation in G2. However, Wesierska-Gadek, *et al.* revealed ROSC activity only at the G2/M transition and accumulation of arrested MCF-7 cells only in the G2 phase. The differences may be attributed to differences in their experimental design, as they exposed MCF-7 cells in a static system to 10μM ROSC for 24 hours [26]. In this study, we tested concentrations of ROSC based on human clinical trial values of a maximum value of 10μM over 1-4 hours, with ROSC clearance within 5 hours, which were below the levels tested in static systems [11]. In this case, dose limiting toxicity of the drug precludes achievement of effective plasma concentrations in humans, which is consistent with the clinical trials. Consequently, ROSC is now being tested in combination therapies [27]. In conclusion, this study demonstrated the application of the dynamic hollow fiber model with controlled pharmacokinetic profiles to simulate clinically relevant dosing schedules of ROSC for treatment of breast tumor cells and the use of a resazurin assay for monitoring cell viability of hollow fiber cell cultures. With this methodology, cells can be recovered for further analysis. The applied hollow fiber model in this study can be used for PK/PD assessment of different anti-neoplastic drugs (single and in combination), with different exposure times against many tumor cell lines.

5. References

[1] Donnelly JG. Pharmacogenetics in cancer chemotherapy: balancing toxicity and response. Ther Drug Monit 2004;26:231-5.

[2] Buschbeck M. Strategies to overcome resistance to targeted protein kinase inhibitors in the treatment of cancer. Drugs R 2006;7:73-86.
[3] Levasseur LM, Slocum HK, Rustum YM, Greco WR. Modeling of the time-dependency of in vitro drug cytotoxicity and resistance. Cancer Res 1998;58:5749-61.
[4] Drusano GL, Bilello PA, Symonds WT, et al. Pharmacodynamics of abacavir in an in vitro hollow-fiber model system. Antimicrob Agents Chemother 2002;46:464-70.
[5] Kirstein MN, Brundage RC, Moore MM, et al. Pharmacodynamic characterization of gemcitabine cytotoxicity in an in vitro cell culture bioreactor system. Cancer Chemother Pharmacol 2008;61:291-9.
[6] Kirstein MN, Brundage RC, Elmquist WF, et al. Characterization of an in vitro cell culture bioreactor system to evaluate anti-neoplastic drug regimens. Breast Cancer Res Treat 2006;96:217-25.
[7] Page B, Page M, Noel C. A new fluorometric assay for cytotoxicity measurements *in vitro*. Int J Oncology 1993;3:473-6.
[8] Gloeckner H, Jonuleit T, Lemke HD. Monitoring of cell viability and cell growth in a hollow-fiber bioreactor by use of the dye Alamar Blue. J Immunol Methods 2001;252:131-8.
[9] Brooks SC, Locke ER, Soule HD. Estrogen receptor in a human cell line (MCF-7) from breast carcinoma. J Biol Chem 1973;248:6251-3.
[10] Soule HD, Vazguez J, Long A, Albert S, Brennan M. A human cell line from a pleural effusion derived from a breast carcinoma. J Natl Cancer Inst 1973;51:1409-16.
[11] Benson C, White J, De Bono J, et al. A phase I trial of the selective oral cyclin-dependent kinase inhibitor seliciclib (CYC202; R-Roscovitine), administered twice daily for 7 days every 21 days. Br J Cancer 2007;96:29-37.
[12] Squatrito RC, Connor JP, Buller RE. Comparison of a novel redox dye cell growth assay to the ATP bioluminescence assay. Gynecol Oncol 1995;58:101-5.
[13] Nakayama GR, Caton MC, Nova MP, Parandoosh Z. Assessment of the Alamar Blue assay for cellular growth and viability in vitro. Journal of Immunological Methods 1997;204:205-8.
[14] Malumbres M, Carnero A. Cell cycle deregulation: a common motif of cancer. Prog Cell Cycle Res 2003;5:5-18.
[15] David-Pfeuty T, Nouvian-Dooghe Y, Sirri V, Roussel P, Hernandez-Verdun D. Common and reversible regulation of wild-type p53 function and of ribosomal biogenesis by protein kinases in human cells. Oncogene 2001;20:5951-63.
[16] Bach S, Knockaert M, Reinhardt J, et al. Roscovitine Targets, Protein Kinases and Pyridoxal Kinase. J Biol Chem 2005;280:31208-19.
[17] Whittaker SR, Walton MI, Garrett MD, Workman P. The Cyclin-dependent Kinase Inhibitor CYC202 (R-Roscovitine) Inhibits Retinoblastoma Protein Phosphorylation, Causes Loss of Cyclin D1, and Activates the Mitogen-activated Protein Kinase Pathway. Cancer Res 2004;64:262-72.
[18] Shapiro GI. Cyclin-Dependent Kinase Pathways As Targets for Cancer Treatment. J Clin Oncol 2006;24:1770-83.
[19] Iseki H, Ko TC, Xue XY, Seapan A, Hellmich MR, Townsend CM,Jr. Cyclin-dependent kinase inhibitors block proliferation of human gastric cancer cells. Surgery 1997;122:187,94; discussion 194-5.

[20] Benson C, Kaye S, Workman P, Garrett M, Walton M, de Bono J. Clinical anticancer drug development: targeting the cyclin-dependent kinases. Br J Cancer 2005;92:7-12.

[21] McClue SJ, Blake D, Clarke R, et al. In vitro and in vivo antitumor properties of the cyclin dependent kinase inhibitor CYC202 (R-roscovitine). Int J Cancer 2002;102:463-8.

[22] Węsierska-Gądek J, Hajek SB, Sarg B, Wandl S, Walzi E, Lindner H. Pleiotropic effects of selective CDK inhibitors on human normal and cancer cells. Biochemical Pharmacology 2008;76:1503-14.

[23] Węsierska-Gądek J, Kramer MP, Maurer M. Resveratrol modulates roscovitine-mediated cell cycle arrest of human MCF-7 breast cancer cells. Food and Chemical Toxicology, 2008;46:1327-33.

[24] Wojciechowski J, Horky M, Gueorguieva M, Wesierska-Gadek J. Rapid onset of nucleolar disintegration preceding cell cycle arrest in roscovitine-induced apoptosis of human MCF-7 breast cancer cells. Int J Cancer 2003;106:486-95.

[25] Pierga JY, Fiavre S, Vera K, Laurence V, Delbaldo C, Bekradda M, Armand JP, Gianella-Borradori A, Dieras V, Raymond E: A phase 1 and pharmacokinetic (PK) trial of CYC202, a novel oral cyclin-dependent kinase (CDK) inhibitor, in patients (pts) with advanced solid tumors. Proc am soc clin oncol 2003;22:abstr 840.

[26] Węsierska-Gądek J, Maurer M, Schmid G. Inhibition of farnesyl protein transferase sensitizes human MCF-7 breast cancer cells to roscovitine-mediated cell cycle arrest. J Cell Biochem 2007;102:736-47.

[27] Appleyard MV, O'Neill MA, Murray KE, et al. Seliciclib (CYC202, R-roscovitine) enhances the anti-tumor effect of doxorubicin in vivo in a breast cancer xenograft model. Int J Cancer 2008;124:465-72.

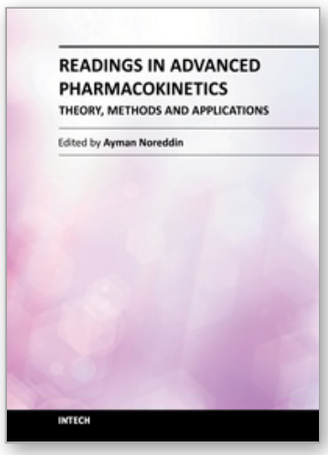

Readings in Advanced Pharmacokinetics - Theory, Methods and Applications

Edited by Dr. Ayman Noreddin

ISBN 978-953-51-0533-6
Hard cover, 378 pages
Publisher InTech
Published online 20, April, 2012
Published in print edition April, 2012

This book, "Readings in Advanced Pharmacokinetics - Theory, Methods and Applications", covers up to date information and practical topics related to the study of drug pharmacokinetics in humans and in animals. The book is designed to offer scientists, clinicians and researchers a choice to logically build their knowledge in pharmacokinetics from basic concepts to advanced applications. This book is organized into two sections. The first section discusses advanced theories that include a wide range of topics; from bioequivalence studies, pharmacogenomics in relation to pharmacokinetics, computer based simulation concepts to drug interactions of herbal medicines and veterinary pharmacokinetics. The second section advances theory to practice offering several examples of methods and applications in advanced pharmacokinetics.

INTECH
open science | open minds

InTech Europe
University Campus STeP Ri
Slavka Krautzeka 83/A
51000 Rijeka, Croatia
Phone: +385 (51) 770 447
Fax: +385 (51) 686 166
www.intechopen.com

InTech China
Unit 405, Office Block, Hotel Equatorial Shanghai
No.65, Yan An Road (West), Shanghai, 200040, China
中国上海市延安西路65号上海国际贵都大饭店办公楼405单元
Phone: +86-21-62489820
Fax: +86-21-62489821

IntechOpen